Acupuncture Exerts Antidepressant Effects in Rats of Chronic Unpredictable Mild Stress: The Involvement of Inflammation in Amygdala and Brain-Spleen Axis

Wenjie Chen
Xiamen University
Yiping Chen
Shanxi University of Traditional Chinese Medicine
Wenjing Cheng
Xiamen University
Peng Li
Shanghai University of Traditional Chinese Medicine
Junliang Shen
Xiamen University
Tao Tong
Shanxi University of Traditional Chinese Medicine
Simin Yan
Xiamen University
Zichun Huang
Xiamen University
Jiawei Li
Xiamen University
Shuqiong Huang
Xiamen University
Xianjun Meng (mengxianjun@xmu.edu.cn)
Xiamen University

Research Article

Keywords: Acupuncture, Depression, Inflammation, Amygdala, Brain-spleen axis, HMGB1/ TLR4 signaling pathway, Systemic immunity

Posted Date: May 17th, 2022

DOI: https://doi.org/10.21203/rs.3.rs-1630267/v1

Abstract

Background

Acupuncture has shown antidepressant effects in rats with chronic unpredictable mild stress (CUMS). However, the mechanisms of antidepressant effects of acupuncture still need to be explored. In the study, acupuncture was applied to a rat depression model of CUMS, high-mobility group box 1(HMGB1) / toll-like receptor 4 (TLR4) and brain-spleen axis were assessed.

Methods

Male Sprague Dawley (SD) rats were exposed to CUMS with two stressors per day for 28 days. In the meantime, manual acupuncture (at GV16 and GV23 acupoints, once every other day) and fluoxetine gavage (2.1 mg/kg, 0.21 mg/mL) were administered daily post-CUMS stressors. Behavioral tests and biological detection methods were conducted in sequence to evaluate depression-like phenotype in rats.

Results

The results showed CUMS induced depression-like behaviors, hyper-activation of HMGB1/TLR4 signaling pathway, elevated inflammation in amygdala and peripheral blood, and hyperactivation of hypothalamic-pituitary-adrenal (HPA) axis. These changes could be reversed by acupuncture to varying extents.

Conclusion

Acupuncture ameliorated depression-like symptoms induced by CUMS, possibly via regulating inflammation mediated by HMGB1/TLR4 signaling pathway in amygdala and peripheral blood circulation, thus improving behavioral outcomes through brain-spleen axis and HPA axis regulation.

Introduction

Depression is an emotional disorder mainly with significant and persistent depressive mood and pleasure deficiency(1). The disease has posed a threat to human health with high prevalence, high recurrence rate and high disability rate(2).

Currently, selective serotonin reuptake inhibitors (SSRIs), particularly fluoxetine, provide better tolerance in patients compared to other antidepressant drugs (ADDs) and are commonly used to treat depression(3, 4). However, SSRIs have been questioned due to many adverse effects, like headache, dizziness, tremor and sexual dysfunction(5, 6), inefficacy in about 50% of patients and heavy financial burden during longtime treatment(7–10). Given this, increasing number of patients are unwilling to take ADDs for treatment. Therefore, natural alternative therapies, such as acupuncture, have been increasingly accepted.

To have acupuncture function adequately, there is a need to further explore the neurobiological underpinnings of acupuncture on depression.

The amygdala plays a critical role in regulating emotional behaviors such as depression(11), learning ability and cognitive function(12, 13). The spleen is a secondary lymphoid organ that plays an important role in generating immune responses. Interestingly, there exists a neuronal pathway, i.e., brain-spleen axis, connecting corticotropin-releasing-hormone (CRH)-expressing neurons in the central amygdala (CeA) and paraventricular nucleus (PVN) of the hypothalamus with the splenic nerve in the spleen(14). It is hypothesized that the brain-spleen axis is an emerging integrative system involved in depression via modulating systemic immunity(14, 15). Additionally, the hypothalamic-pituitary-adrenal (HPA) axis is the primary neuroendocrine hormonal pathway by which the central nervous system (CNS) regulates the immune system(16). Since the underlying initiation and development mechanisms of depression has not been elucidated so far, these studies may shed some light on it.

Increasing number of evidences indicate that immune responses, with inflammation and neuroinflammation included, directly affects neurodegeneration in CNS, which is closely related to the development of brain and psychiatric disorders(17, 18). High-mobility group box 1 (HMGB1) is critical in inducing and promoting the occurrence of inflammation and neuroinflammation(19, 20). Studies indicate that HMGB1 can be up-regulated when stressed, accompanied with the increasing expression of its receptor in toll-like receptor 4 (TLR4)(21, 22). TLR4 is an immune regulator of neuroimmune and neuroendocrine interactions in stress and depression(23). After HMGB1 binds TLR4, inflammatory responses in the brain and periphery are induced(24–26).

Acupuncture is an effective alternative therapy for depression, with fewer adverse effects and lower cost. Manual acupuncture combined SSRIs treatment was reported to ameliorate symptoms and quality of life for patients with moderate to severe depression(27). Some researchers found that acupuncture could maintain internal homeostasis through acupuncture at normal rats(28). Additionally, acupuncture has a general lower risk of adverse effect than that in ADDs(29). Though acupuncture plays a certain role in antidepressant, what is to be further studied is how acupuncture works mechanistically(30), especially how acupuncture affects inflammation, brain-spleen axis and HPA axis. Previous studies show that acupuncture corrects pro-inflammatory factors in specific brain regions of rats induced by CUMS as fluoxetine did(31). Further, electroacupuncture (EA) reverses inflammation and neuroinflammation in rodents' hippocampi(32), and depresses hyperactivity of HPA axis(33) in CUMS rats. However, there are a few studies focusing on the effects of acupuncture on the brain-spleen axis.

Our previous studies illustrate that acupuncture may reverse depression-like behavior by regulating intestinal microbes, neurotransmitters(34), NO-cGMP signaling pathway in hippocampus and plasma(35), and reducing oxidative stress products via regulating the Nrf2/HO-1 signaling pathway(36). Others have explored the effects of acupuncture on rodents' brain regions associated with depression other than the hippocampus, such as the cingulate cortex, motor cortex, insular cortex, thalamus, and hypothalamus(30, 37). However, inflammation in amygdala, brain-spleen axis, and the relationship

among them in the development of depression have not been clearly elucidated. Further, it is still unknown how acupuncture works on depression via the above possible mechanism.

Herein, we investigated the effects of simultaneous stimulation of acupuncture at *Fengfu* (GV16) and *Shangxing* (GV23) acupoints in rats exposed to CUMS stressors on HMGB1-induced inflammation in the amygdala and peripheral blood. This research provides insight into the integrative biology between the HPA axis and the brain-spleen axis.

Material And Methods

Animals

Forty specific-pathogen-free (SPF) male Sprague Dawley (SD) rats (130-150g) were obtained from Shanghai SLAC Laboratory Animal Co., Ltd. (qualified No. SCXK 2017-0005, Shanghai, China), and raised in the Animal Laboratory of Medical College of Xiamen University with a SPF laboratory environment. They were housed in plastic cages (3 or 4 rats per cage) with dry corncob padding with temperature of 23±2°C and relative humidity of 65±5%, exposed to light from 08:00 to 20:00 daily, and given free access to adequate water and food (except when indicated). All experiments and protocols complied with international animal experimental ethics and requirements, and were approved by the Animal Ethics Committee of Xiamen University (license No. XMULAC20210062).

Groups

All animals were allowed to adapt to the new environment for 7 days before the conduction of formal experiments. Then rats were weighed and 36 of 40 rats were selected to ensure a consistent baseline. Afterwards, the 36 rats were randomly divided into four groups (9 rats in each group): control group (CON), chronic unpredictable mild stress (CUMS) group (CUMS), acupuncture + CUMS group (AP), and fluoxetine + CUMS group (FX). Over the next 28 days, except for rats in the control group, fed as adaptive feeding, other rats were performed with CUMS (Supplementary Table 1), and the latter two groups were treated with acupuncture (20 min per time, once every other day) and intragastric fluoxetine (once daily) respectively between 14:00 and 15:00 p.m. when CUMS procedure finished(38). See the Figure 1A for all specific procedures.

Chronic unpredictable mild stress model procedure

The CUMS protocol, originally developed by Paul Willner, has been a widely used, reliable, and effective rodent model of depression(39, 40). The protocols were selectively referred to the study of Franklin and her colleagues(25) with minor changes. Rats in CUMS, AP and FX groups were all exposed to CUMS protocols that consisted of a random combination of two stressors per day lasting for 28 days when the same stressors not used again in 3 days (Supplementary Table 1). To ensure the unpredictability of molding, the same stressor did not appear continuously. Survival was closely monitored throughout the procedure.

Intervention procedure

Manual acupuncture

Manual acupuncture was administered at the *Fengfu* (GV16) and *Shangxing* (GV23) acupoints with location referring to Experimental Acupuncture Science(41) and shown in Figure 1B. *Fengfu* lies in the concave joint of the pillow bone top at the back of the pillow bone, i.e. the middle point of the back edge of both ears. *Shangxing* is located at the midpoint of the *Baihui* (GV20, the intersecting point of the tip of the two ears and anterior midline) and the *Yintang* (GV29, at the midpoint between the two medial ends of the eyebrow). Disposable aseptic steel filiform needles (0.25 mm diameter, 13 mm length; Hanyi, Changchun Aikang Medical Instrument Co., Ltd) were inserted into the two acupoints of the skin, with an oblique angle (30°) towards apex nasi of each rat, and the depth of 5 mm, and were twisted at a frequency of 100 times/min and an amplitude of -90 to 90 degree for 5 s. To keep the filiform needles in right location, we prepared an auxiliary needling cloth headset for rat (patent No. ZL2019224218143) avoiding rats' tempering in advance (Figure 1B) and then kept it on rats' heads for 20 min. The needles were twisted another 5 s at same frequency and amplitude as mentioned above. Acupuncture procedure was conducted in each rat once every other day for 28 days.

Fluoxetine gavage

Rats in FX group were intragastrically administered with fluoxetine (2.1 mg/kg with the concentration of 0.21 mg/mL distilled water; PHR1394-1G, Sigma-Aldrich, USA) at a volume of 10 mL/kg once a day for 28 days(34).

Behavioral testing

Rats' body weight assessing their appetite and nutritional status were measured on days 0, 7, 14, 21, and 28. All rats were subjected to behavioral tests on days 29 (OFT), 30 (EPM), 31 (FST), and 32-34 (SPT) after molding and intervention procedure.

Open field test (OFT)

The OFT is designed for the evaluation of spontaneous locomotor activity in rodents(42). A black and brightly lit box (100 cm × 100 cm × 40 cm, length × width × height) with the bottom equally divided into sixteen grids (four grids in the center called the central zone, surrounded by twelve peripheral zones, allowing to evaluate the exploration of internal and external area) was prepared. Firstly, each rat was gently placed into the center for 5 min when the spontaneous moving of rats was videotaped by a tracking system (Smart 3.0). Then the number of grids crossed for the assessment of rats' locomotor activity(43) (forelegs and one hind leg of an animal in one grid for one crossing to be accounted) as well as defecation times evaluating the level of depression and anxiety(44) were written down by two observers blind to grouping. Lastly, each rat was put back its home cage and the box was thoroughly cleaned with 75% ethanol and kept dry between trials.

Elevated plus maze test (EPM)

The EPM is originally developed to evaluate anxiety-like behavior of rodents(45). The test was performed in a black apparatus consisted of two opposite open arms (50 cm × 10 cm), a central area (10 cm × 10 cm) and two opposite closed arms (50 cm × 10 cm × 40 cm), elevated 60 cm from the ground. Based on rodents' exploratory nature(46), animals were placed in the central area where the arms crossed, facing the open arms where each rat could see over the edge and allowed to explore for 5 min. Exploratory behavior of each rat was monitored by a high-resolution infrared camera, connected with a tracking system (Smart 3.0), above the apparatus. Then time spent in the open and closed arms(47) were measured and each rat was returned back to their home cages. The apparatus was cleaned with 75% ethanol and allowed time to dry prior to the next run.

Forced swimming test (FST)

Immobility in FST reflects behavioral despair in rodent(48). We made minor changes and recorded immobility duration total (%) for detection. Briefly, all rats were placed into a plastic cylinder (diameter = 21 cm, height = 60 cm) filled with freshwater (depth = 45 cm; 23 ± 1℃). Rats' immobility time was followed and recorded by a numeric tripod-fixed camera connected with a tracking system (Smart 3.0) through a 5 min testing session. The immobility was determined by the absence of movement except slight actions to keep the head above the water and maintain balance. Immobility duration in a total 5 min was calculated.

Sucrose preference test (SPT)

SPT has been widely applied to assess anhedonia and depression(49). The sucrose powder (R015039) was purchased from Rhawn (Yien Chemical Technology Co., Ltd) in Shanghai, China. Firstly, there was a habituation period of 1% sucrose solution for 48 h, when rats were provided with two bottles of 1% sucrose solution (250 g bottle weight, the same below) for the first 24 h, and a bottle of pure water and a bottle of 1% sucrose solution for the second 24 h with exchanging location every 12 h to avoid side-bias. Deprivation of water and food was conducted for 12 h. Afterwards, animals went through formal testing for 12 h(34), during which they were given free access to food and two bottles of different fluid as in the second 24 h and the consumption of pure water and 1% sucrose solution measured by the weight loss of corresponding bottles. Sucrose preference rate of each rat was calculated as follows: sucrose preference rate (%) = sucrose intake/total fluid consumption×100%.

Sample collecting procedure

Rats were euthanized by intraperitoneally injecting 10% chloral hydrate (3 mL/kg)(50) combined with immediate bloodletting to gather amygdaloid nucleus, spleens and blood from the abdominal aorta. Blood samples were collected in blood collection tubes with separating gel and coagulant (YA1271, Solarbio, Beijing, China), allowed to stand at 4℃ for over 4 h and centrifuged at 3000 rpm for 15 min to collect serum. Amygdaloid nucleus was promptly separated from the brain. Spleens were removed, and

their weight and length were measured. All samples collected except blood were quickly frozen in liquid nitrogen and then put at -80℃ for subsequent biochemical analysis.

Immunofluorescence (IF)

Brain matrix was cut into 2 mm coronal sections. After fixed in 4% paraformaldehyde, amygdala tissue was embedded in paraffin and sliced into 5-μm-thick sections. Amygdala sections were deparaffinized and rehydrated, then treated with EDTA antigen retrieval buffer (pH 8.0) to retrieve antigen. After that, the following steps were performed: antibody blocking, incubated with primary antibody (HMGB1 antibody, 1:100, GB11103; IBA1 antibody, 1:100, GB13105-1; GFAP antibody, 1:100, GB11096) followed by secondary antibody (Cy3 conjugated Goat Anti-Rabbit IgG (H+L), 1:300, GB21303), nucleus counterstained by DAPI (G1012), incubated with spontaneous fluorescence quenching reagent, and PBS (pH 7.4) washing three times, 5-min each between steps. Lastly, slips were covered with anti-fluorescence solution and observed under a confocal microscope (×200 magnification, Nikon DS-U3, Tokyo, Japan) to search for the presence of immune-positive neurons and collect images. The %area of HMGB1, IBA1 and GFAP (portion of positive area in a total visual area) was calculated using the “area fraction” in Fiji ImageJ software (National Institutes of Health, Bethesda, MD)(51). There were 3 samples in each group for immunofluorescence staining. A total of 3 nonoverlapping visual fields in amygdala were randomly selected in each section respectively. Quantification was carried out by experimenters blinded to the study. Mean value of %area obtained under three different visual fields of one section stood for the %area of the section. The antibodies and reagents used for IF were all purchased from Servicebio company in Wuhan, China.

Western blotting (WB)

Tissue samples (100 mg per rat) were ground and centrifuged for collecting supernatants form tissue homogenates. After that, protein concentration was determined by a BCA protein assay kit (QB214754, Thermo Scientific, MA, USA). Proteins were separated on prepared 10% SDS-PAGE gel, and then separated proteins were transferred to a polyvinylidene fluoride (PVDF) membrane (K5NA8023B, Amersham, Sweden) by electrophoresis. After transfer, the PVDF membrane was soaked in a blocking reagent containing 5% nonfat dry milk and incubated at a room temperature for 1h, with corresponding primary antibodies (anti-HMGB1, 1: 1000, 10829, Proteintech, Chicago, USA; anti-TLR4, 1: 1000, 19811, Proteintech; anti-NKG2D, 1: 1000, Ab203353, Abcam, Cambridge, USA; anti-β-actin, 1: 1000, 20536, Proteintech) and shaken at 4 ℃ till next day. After washed, the membrane was incubated with HRP-labeled rabbit secondary antibody (1:5000, SA00001, Proteintech) solution at room temperature for 1 h. Washed again, the membrane interacted with enhanced chemiluminescent to develop color, and was exposed and developed in a dark room. Protein band density was quantified by ImageJ software (National Institutes of Health, Bethesda, MD). The gray value of the target strip was divided by the gray value of the internal parameter (β-actin). Lastly, the ratios in other groups were compared with that of control group respectively for normalization and shown in the results. Every sample was detected 3 times, and cropped strips were shown in figures. The original strips were provided as supplementary materials.

Reverse transcription-polymerase chain reaction (RT-PCR)

Before detection, mRNA coding sequences of HMGB1, TLR4 and NKG2D were obtained from Consensus Coding Sequence database of the National Center for Biotechnology Information (NCBI). Based on these sequences, specific primers of proteins were designed as Supplementary Table 2. Firstly, tissue samples (50 mg per rat) were ground, lysed with 1 mL of Trizol reagent for extraction of total RNA under the instructions of RNA extraction kit (RN03, Aidley Biotechnology Co. Ltd, China), including quantifying the concentration of RNA by measuring optical density value (OD value) with ultramicro spectrophotometer (NanoVue Plus, General Electric Company, Boston, USA) and the concentration range was 500-2000 ng/μL. Secondly, 1 μL of RNA was reversely transcribed to cDNA using Oligo (dT). Then 25 ng of the cDNA was used for the preparation and amplification of PCR system according to the instrument of reverse transcription kit (FSQ-101, TOYOBO, Japan). Finally, 1.5 μL of PCR product was detected by electrophoresis (120 V) on 1% agarose gel for 10 min, and the gel was imaged for assessing the integrity of RNA. Temperature cycle was conducted as following conditions: 94 ℃, 5 min; denaturation temperature 94℃, 30 s; annealing temperature 56 ℃, 30 s; extension temperature 72 ℃, 30 s; 72 ℃, 10 min; 4 ℃, 5 min; one cycle includes denaturation, annealing and extension; there were 35 cycles conducted. ImageJ software (National Institutes of Health, Bethesda, MD) was used for gray-scale analysis, where target mRNA result was compared with that of referring β-actin.

Enzyme-linked immunosorbent assay (ELISA)

Serum and supernatants from amygdala homogenates were collected for ELISA. Standard dilution solution of various concentration was prepared previously. All protocols of kit utilization were conducted under guidance of the manufactures of corresponding ELISA kits. Except for TNFα (JL17113, Jianglai biology, Shanghai, China) and CORT (H094, Jiancheng, Nanjing, China) ELISA kit, others (CRP, E-EL-R0506c; IL6, E-EL-R0015c; IL1β, E-EL-R0012c; CRH, E-EL-R0270c; ACTH, E-EL-R0048c) were all products of Elabscience company in Wuhan, China. After that, the OD value of each well was measured at a wavelength of 450 nm in 15 min, and the quantities of serum and supernatants from amygdala homogenates were calculated according to the standard curve.

Statistical analysis

Normality and homogeneity of variance in groups were confirmed before data analysis. One-way analysis of variance (ANOVA) was performed when data confirmed to normality and homogeneity of variance. Brown-Forsythe test and Welch ANOVA tests were applied when the variance was uneven. Nonparametric test (Kruskal-Wallis test) was applied when data did not conform to normal. Dunnett's method was used for multiple comparisons. Data in figures are expressed as mean ± standard error of the mean ($\bar{x} \pm s$). A P value <0.05 was of statistical significance. All data were analyzed using GraphPad Prism 8.2.0 (GraphPad software Inc., San Diego, California, USA).

Results

Acupuncture ameliorated depression-like symptoms in CUMS rats.

Behavioral test results were shown in Fig. 1 and Fig. 2. Compared with the control group, our results showed significant reduction in rats' weight growth ($F_{(3.000, 21.32)} = 32.38$, $P < 0.0001$, Fig. 1C and D), sucrose intake ($F_{(3.000, 27.43)} = 13.58$, $P < 0.05$, Fig. 2A), number of grids crossed ($F_{(3.000, 19.21)} = 12.74$, $P < 0.001$, Fig. 2C) and time in open arms ($P < 0.01$, Fig. 2G) but more immobility duration total ($F_{(3.000, 13.48)} = 10.96$, $P < 0.01$, Fig. 2B), fecal excretion times ($F_{(3.000, 23.83)} = 12.47$, $P < 0.01$, Fig. 2F), and time in closed arms ($P < 0.001$, Fig. 2H) after CUMS. No significance between intervention groups and control one ($P > 0.05$). The alteration of activity track of rats in OFT and EPM have been also shown in Fig. 2D and E. Whereas, compared with CUMS group, acupuncture group showed more weight gain from the 21st day ($F_{(3.000, 21.32)} = 32.38$, $P < 0.05$, Fig. 1C and D), sucrose consumption ($F_{(3.000, 27.43)} = 13.58$, $P < 0.01$, Fig. 2A), grids crossed($F_{(3.000, 19.21)} = 12.74$, $P < 0.01$, Fig. 2C), and time in open arms ($P < 0.001$, Fig. 2G), but less immobility duration total ($F_{(3.000, 13.48)} = 10.96$, $P < 0.05$, Fig. 2B), fecal excretion times ($F_{(3.000, 23.83)} = 12.47$, $P < 0.001$, Fig. 2F) and time in closed arms ($P < 0.01$, Fig. 2H). There was no statistical significance between groups of acupuncture and fluoxetine ($P > 0.05$). The above indicated a beneficial effect of acupuncture on depression-like behavior of CUMS rats as that of fluoxetine.

Acupuncture depressed activation of HMGB1/ TLR4 signaling pathway in amygdala of CUMS rats.

HMGB1/ TLR4 signaling pathway in amygdala were mainly detected with WB analyses and RT-PCR as illustrated in Fig. 3 and Supplementary Table 3. HMGB1 was also visualized by IF. Overall, compared with the control, protein and mRNA concentrations of HMGB1($F_{(3.000, 7.019)} = 8.568$, $P < 0.05$, Fig. 3B; $F_{(3.000, 6.591)} = 10.36$, $P < 0.01$, Fig. 3E) and TLR4 ($F_{(3.000, 4.575)} = 5.003$, $P = 0.0678$, Fig. 3C; $P < 0.05$, Fig. 3F) in amygdala were increased in CUMS group. There was no statistical significance between intervention groups and control group ($P > 0.05$). These increased levels in the pathway were reduced respectively by acupuncture to varying extents: protein and mRNA levels of HMGB1($F_{(3.000, 7.019)} = 8.568$, $P = 0.0844$, Fig. 3B; $F_{(3.000, 6.591)} = 10.36$, $P = 0.0814$, Fig. 3E) and TLR4 ($F_{(3.000, 4.575)} = 5.003$, $P = 0.2980$, Fig. 3C; $P = 0.6388$, Fig. 3F). In addition, the %area of HMGB1 was increased visibly ($F_{(3.000, 4.901)} = 15.54$, $P = 0.0541$, Fig. 3G and H) after stress but reduced by acupuncture ($F_{(3.000, 4.901)} = 15.54$, $P < 0.05$, Fig. 3G and H). All the above indexes had no statistical significance between acupuncture groups and fluoxetine groups ($P > 0.05$). Though the effect of acupuncture on TLR4 was light, there existed a trend of alleviating inflammation via HMGB1/ TLR4 signaling pathway under acupuncture intervention in general.

Acupuncture reversed structural alteration and elevated inflammation in spleens of CUMS rats.

We measured the length and weight of spleens in rats in Fig. 4A-C. Rats under CUMS condition had shorter ($F_{(3.000, 14.16)} = 6.393$, $P < 0.01$, Fig. 4C) and lighter ($F_{(3.000, 13.35)} = 4.284$, $P = 0.0662$, Fig. 4B) spleens than they in CON. Acupuncture could improve the length ($F_{(3.000, 14.16)} = 6.393$, $P = 0.2586$, Fig. 4C) and weight ($F_{(3.000, 13.35)} = 4.284$, $P = 0.1115$, Fig. 4B) of spleens marginally. No significance was

observed between groups of intervention and control ($P > 0.05$), or between groups of acupuncture and fluoxetine ($P > 0.05$).

Further investigations of HMGB1/TLR4 pathway and pro-inflammatory factors in spleens were measured with WB (Fig. 4D-H and Supplementary Table 3). Compared with the control, the protein concentration of HMGB1($F_{(3, 8)} = 9.370$, $P < 0.01$, Fig. 4E), TLR4 ($F_{(3,8)} = 11.56$, $P < 0.001$, Fig. 4G), IL1β ($F_{(3, 8)} = 10.77$, $P < 0.01$, Fig. 4H) and TNFα ($F_{(3,8)} = 10.11$, $P < 0.01$, Fig. 4F) were significantly elevated in CUMS group. No statistical significances between intervention groups and control group were observed ($P > 0.05$). These increased levels were reduced respectively by acupuncture: HMGB1 ($F_{(3, 8)} = 9.370$, $P < 0.05$, Fig. 4E), TLR4 ($F_{(3,8)} = 11.56$, $P < 0.05$, Fig. 4G), IL1β ($F_{(3, 8)} = 10.77$, $P = 0.0549$, Fig. 4H) and TNFα ($F_{(3,8)} = 10.11$, $P < 0.05$, Fig. 4F). There was no significance between groups of acupuncture and fluoxetine ($P > 0.05$). These indicated acupuncture could affect spleens both functionally and structurally, similarly fluoxetine.

Acupuncture decreased pro-inflammatory factors in amygdala and serum of CUMS rats.

To explore whether acupuncture reduced inflammation, pro-inflammatory factors, such as IL6, IL1β, TNFα and CRP in amygdala and serum were detected with ELISA. As shown in Fig. 5A-H, CUMS markedly increased the levels of CRP ($F_{(3.000, 14.56)} = 6.496$, $P < 0.05$, Fig. 5A; $F_{(3.000, 19.68)} = 10.27$, $P < 0.01$, Fig. 5E), IL6 (6; $F_{(3.000, 19.01)} = 14.16$, $P < 0.001$, Fig. 5B; $F_{(3.000, 13.53)} = 16.69$, $P < 0.01$, Fig. 5F), TNFα ($F_{(3.000, 19.14)} = 13.81$, $P < 0.001$, Fig. 5C; $F_{(3.000, 17.00)} = 23.93$, $P < 0.001$, Fig. 5G) and IL1β ($F_{(3, 20)} = 7.590$, $P < 0.001$, Fig. 5D; $P < 0.001$, Fig. 5H) in amygdala and serum. Acupuncture could significantly decrease the level of IL6 ($F_{(3.000, 19.01)} = 14.16$, $P < 0.01$, Fig. 5B), TNFα ($F_{(3.000, 19.14)} = 13.81$, $P < 0.05$, Fig. 5C) and IL1β ($F_{(3, 20)} = 7.590$, $P < 0.05$, Fig. 5D) in amygdala, CRP ($F_{(3.000, 19.68)} = 10.27$, $P < 0.01$, Fig. 5E), IL6 ($F_{(3.000, 13.53)} = 16.69$, $P < 0.05$, Fig. 5F), TNFα ($F_{(3.000, 17.00)} = 23.93$, $P < 0.01$, Fig. 5G) and IL1β($P < 0.05$, Fig. 5H) in serum. Acupuncture did not affect CRP levels ($F_{(3.000, 14.56)} = 6.496$, $P = 0.1435$, Fig. 5A) in amygdala. There was no significance between the groups of control and intervention ($P > 0.05$), or between the groups of acupuncture and fluoxetine ($P > 0.05$). These alterations indicated that acupuncture reduced inflammatory environments in peripheral blood and amygdala, similar to fluoxetine positive controls.

Acupuncture depressed the hyperactivation of HPA axis in CUMS rats.

We also detected the concentrations of CRH, ACTH and CORT using ELISA to test the activation of HPA axis. In Fig. 6A-F, the expression of CRH ($F_{(3.000, 18.83)} = 7.954$, $P = 0.0517$, Fig. 6A; $F_{(3, 20)} = 9.871$, $P < 0.001$, Fig. 6D), ACTH ($F_{(3, 20)} = 2.591$, $P < 0.05$, Fig. 6B; $F_{(3, 20)} = 8.190$, $P < 0.001$, Fig. 6E) and CORT ($F_{(3.000, 15.81)} = 7.659$, $P < 0.01$, Fig. 6C; $F_{(3, 20)} = 9.995$, $P < 0.001$, Fig. 6F) in amygdala and serum were elevated in CUMS rats. There was no significance between control groups and two intervention groups ($P > 0.05$). Interestingly, acupuncture could reduce the level of CRH ($F_{(3.000, 18.83)} = 7.954$, $P < 0.01$, Fig. 6A; $F_{(3, 20)} = 9.871$, $P < 0.01$, Fig. 6D) in amygdala and serum, ACTH ($F_{(3, 20)} = 8.190$, $P < 0.05$, Fig. 6E) and CORT ($F_{(3, 20)} = 9.995$, $P < 0.01$, Fig. 6F) in serum and CORT ($F_{(3.000, 15.81)} = 7.659$, $P = 0.0623$, Fig. 6C) in amygdala. No significance between acupuncture group and fluoxetine group could be seen from the

above indicators ($P > 0.05$). These indicated that acupuncture depressed the hyperactivation of HPA axis of CUMS rats as fluoxetine did.

Acupuncture changed the activation of microglia and astrocytes in amygdala of CUMS rats.

To visualize the expression of IBA1 and GFAP in amygdala, immunofluorescence was performed. As Fig. 7 and Supplementary Table 3 show, compared with the control group, the %area of IBA1 and GFAP in the model group were ($F_{(3, 8)} = 2.808$, $P = 0.5632$, Fig. 7C) and ($F_{(3, 8)} = 2.380$, $P = 0.2659$, Fig. 7D); compared with the model group, the %area of IBA1 and GFAP in AP group were $P = 0.2084$ and $P = 0.1435$, respectively. There existed the same effect between groups of acupuncture and fluoxetine ($P > 0.05$).

Acupuncture ameliorated immunity depression in spleens of CUMS rats.

To probe into the effects of acupuncture on immune response in spleen, the concentration of NKG2D was detected using WB and RT-PCR as demonstrated in Fig. 8 and Supplementary Table 3. As we can observe, when compared with the control, the expression of NKG2D protein ($F_{(3.000, 4.674)} = 17.04$, $P < 0.05$, Fig. 8C) and its mRNA ($P < 0.05$, Fig. 8D) were both obviously decreased by CUMS. Acupuncture slightly reversed the increased protein level of NKG2D ($F_{(3.000, 4.674)} = 17.04$, $P = 0.0865$, Fig. 8C), but did not affect its mRNA ($P = 0.5227$, Fig. 8D). No significances between groups of acupuncture and fluoxetine ($P > 0.05$) were observed.

Discussion

We conducted a model of depression induced by 28-days of CUMS stressors in rats to investigate the mechanisms involved. Our results indicated acupuncture at GV16 and GV23 acupoints could reverse inflammation and depression-like behaviors.

Acupuncture has been used for the treatment of neuropsychiatric disorders, such as depression. GV16 and GV23 are two of acupoints(52), lying in Governor Vessel (GV) which is capable of gathering and conveying energy to brain for energizing the whole body(53). Additionally, they are all on the top, available of adjusting brain function(54). Some researchers reviewed a high use frequency of the two points in clinical trials(55). In the theory of traditional Chinese medicine, there exists synergy and complementarity in simultaneous stimulation at different acupoints, which can also enhance safety and curative effect(56). Our previous studies found that acupuncture at an acupoint combination of GV23 and PC7 or a combination of GV16 and GV23, exerts antidepressant effect in CUMS rats(34–36). Accordingly, GV16 and GV23 were selected and applied in this study. Fluoxetine exerted anti-inflammatory and antioxidant effect whether in patients with depression(57) or in rats of chronic social isolation model of depression(58). Given these, we took fluoxetine as a positive control to better investigate antidepressant mechanisms of acupuncture. The results showed that acupuncture at GV16 and GV23 effectively reversed depression-like phenotypes in CUMS rats as fluoxetine did. Considering that there was no significant difference between groups of control and control + fluoxetine or between

groups of control and control + acupuncture based on previous work of us and other researchers(59), neither a control + acupuncture nor a control + fluoxetine was performed in these studies following the 3R principle of animal welfare.

Previous reports indicate depression-like behaviors and pro-inflammatory cytokines are observed in rodents under chronic stress, which is consistent with elevated serum inflammatory factors in patients with depressive disorders(60–62). The CUMS model is a popular and reliable rodent model of depression(63). Core symptoms of depression induced by the CUMS model, were detected by OFT, EPM, FST and SPT. Our study showed increasing levels in immobility duration, defecation times and time in closed arms but decreased weight growth, number of grids crossed, sucrose preference rate and time in open arms in CUMS rats. These indicated that CUMS induced poor autonomy ability, strong anhedonia, despair and depression in rats. These changes were all improved significantly by acupuncture as fluoxetine did. Therefore, acupuncture might begin to work from the 21st day of administration based on body weight result. This may prove that there is a gradually ameliorating effect of acupuncture on depression-like behaviors, and that a longer timepoint of intervention of acupuncture may be required to treat depression clinically.

Neurobiological abnormalities play essential roles in modulating depression, including alterations in inflammation, the HPA axis, neurogenesis, monoaminergic systems and interaction among them(64, 65). Neurons expressing CRH in CeA and PVN of the hypothalamus end in the splenic nerve of the spleen. Interestingly, when CRH-expressing neurons are activated in the amygdala the splenic nerve could also be activated, stimulating the formation of antibody producing plasma cell differentiation(14). These studies suggest a possible pathway between brain-spleen axis and humoral immunity(14, 66). Amygdala, a key brain region associated with emotion, learning and memory, is closely related to the development of depression(12). Therefore, amygdala was selected as the target brain region in the study to explore the inflammation induction in amygdala and peripheral blood.

HMGB1, a nucleoprotein for DNA replication, transcription and repair, is released into cytoplasm and involves in the initiation of inflammation and neuroinflammation under stress condition(67). HMGB1 can silence stress-induced inflammatory diseases after being inhibited(24, 26). HMGB1 also plays a role as a damage associated molecular pattern (DAMP), capable of binding to its pattern recognition receptors (PRRs) and thus leading to inflammation and neuroinflammation when released(20). TLR4 is one of its PRRs(20). Besides, HMGB1 could promote the action of other DAMPs as an internal cellular stress, thus further increasing inflammation and neuroinflammation(25). Previous studies reported that the expression of HMGB1 and TLR4 were both upregulated in the brains of patients with depression(21) and in stress-induced rats(68). In this study, the expression of HMGB1 and TLR4 were elevated under CUMS in rats' amygdalae and spleens with downregulating effects of acupuncture.

HMGB1 binding to TLR4 promotes a series of inflammatory response, such as the upregulation of interleukin 1 beta (IL1β) and tumor necrosis factor alpha (TNFα)(24, 26). Similar to our study, inflammation is thought to positively correlate with depression. Particularly the upregulation of pro-

inflammatory factors, such as IL1β, IL6, TNFα and C reactive protein (CRP), participate in the occurrence of depression as reported in both clinical(69) and experimental research(70, 71). We observed that the expression of IL1β, IL6, TNFα and CRP increased in the amygdala and serum of rats post CUMS as the previous. Additionally, increased expression of IL1β and TNFα was also observed in rats' spleens. Yet these changes were all corrected by acupuncture and fluoxetine. Furthermore, pro-inflammatory cytokines tend to activate glial cells to expand inflammation. In the study, ionized calcium binding adaptor molecule 1 (IBA1) and glial fibrillary acidic protein (GFAP) were used as the former(72, 73) to mark the activated phenotype of microglia and astrocytes, respectively. We observed increased trends of %area (the portion of positive area in a total vision) of microglia and astrocytes in model rats, which were downregulated by acupuncture slightly. Although significance was not reached, we suspected, the small sample size might account for it.

PVN, one end of brain-spleen axis, is a critical neuroendocrine organ in the activation of HPA axis(74). Meanwhile, the CRH-expressing neurons in CeA may affect HPA axis and exert their stress capacity by affected CRH. Reports demonstrate increasing mRNA of CRH in amygdala of rats under stress(75), similar to our study. Furthermore, the level of adrenocorticotropic hormone (ACTH) and corticosterone (CORT) in amygdala and serum were detected and are both important components in HPA axis. The HPA axis is a primary hormonal pathway by which the CNS regulates the immune system, through the hormones of the neuroendocrine stress response(16). The activity of HPA axis was reflected by an increased concentration of CORT in serum(76), and sustained release of pro-inflammatory factors may give rise to its expression levels based on previous report(77)and our results. Although there are few reports about ACTH or CORT in amygdala, our report results indicated similar trends of the HPA axis in the amygdala and the peripheral blood, the details of which require further studies. In line with this, some researchers insert ACTH analogues into amygdala and find that (ACTH) directly acts on amygdala neurons and down-regulates the expression of CRH gene(78, 79).

However, it is worth noting that HPA hyperactivation may in turn disrupt the normal functions of the glucocorticoid receptor (GR), and thus increasing the levels of anti-inflammatory cytokines and decreasing the levels of pro-inflammatory cytokines to protect the body from more inflammatory damage(80, 81). This may be why we observed natural killer group 2 member D (NKG2D) reduced expression levels, which is a critical molecule activating peripheral immune response(82, 83). We found that NKG2D acted as a non-specific cytotoxic marker of leukocytes and was reduced in CUMS, suggesting leukocyte subset reduction and potential deficiency. Furthermore, our results indicated that rats under CUMS had shorter and lighter spleens, which might indicate impaired immune function(84). Importantly, acupuncture could reverse these changes. Chronic stress can induce not only HPA axis hyperactivation but also immune suppression(85–87). In addition, the time of collecting samples was 6 days post-CUMS, which is when we observed the hyperactivation of HPA axis(88). This may be due to continuous TLR4 activity post-stress removal, a process that requires further studies(23).

Conclusions

This study indicated that simultaneous stimulation of acupuncture at GV16 and GV23 can exert antidepressant effects mainly by inhibiting inflammation via HMGB1/TLR4 signaling pathway in the brain-spleen axis (Fig. 9). Certainly, there are some shortages in our research, for example the small sample size and exploration of acupuncture on brain-spleen axis is still rudimentary. Nonetheless of these shortcomings, we report CUMS-induced stress in rats results in elevated depressive behaviors and inflammation, that could be successfully treated with acupuncture.

Abbreviations

CUMS
chronic unpredictable mild stress
HMGB1
high mobility group box 1
TLR4
toll-like receptor 4
HPA
hypothalamic-pituitary-adrenal
CRH
corticotropin-releasing hormone
ACTH
adrenocorticotropic hormone
CORT
corticosterone
CRP
C reactive protein
IL6
interleukin 6
IL1β
interleukin 1β
TNFα
tumor necrosis factorα
GFAP
glial fibrillary acidic protein
IBA1
ionized calcium binding adaptor molecule 1
NKG2D
natural killer group 2 member D
GV
Governor Vessel
PC

Pericardium Meridian
CeA
central amygdala
PVN
paraventricular nucleus
DAMP
damage associated molecular pattern
PRR
pattern recognition receptor
OFT
open field test
EPM
elevated plus maze test
FST
forced swim test
SPT
sucrose preference test
IF
immunofluorescence
WB
western blotting
RT-PCR
reverse transcription-polymerase chain reaction
ELISA
enzyme-linked immunosorbent assay.

Declarations

Ethical Approval

and Consent to participate

Consent for publication

Not applicable.

Competing interests

The authors declare that there is no conflict of interest.

Funding

The study was supported by grants from the Shenzhen Science and Technology Program (No. JCYJ20210324121800002).

Authors' Contributions

Every author participated in the designing, conduction and data collection of the study. WC and YC contributed to the experimental conduction, results interpretation. WC finished manuscript writing. JS and TT performed data analysis. ZH, JL and SY assisted in the experimental conduction. XM, PL, WC and SH made revisions to the manuscript. XM approved the final manuscript.

Acknowledgments

This study was supported by the Shenzhen Science and Technology Program (No. JCYJ20210324121800002) and the Innovation and Entrepreneurship Club of the Department of Traditional Chinese Medicine of Xiamen University.

References

1. Hedegaard H, Johnson RL. An Updated International Classification of Diseases, 10th Revision, Clinical Modification (ICD-10-CM) Surveillance Case Definition for Injury Hospitalizations. Natl Health Stat Report. 2019(125):1–8.
2. Global Burden of Disease Study C. Global, regional, and national incidence, prevalence, and years lived with disability for 301 acute and chronic diseases and injuries in 188 countries, 1990–2013: a systematic analysis for the Global Burden of Disease Study 2013. Lancet. 2015;386(9995):743–800.
3. Anderson IM, Nutt DJ, Deakin JF. Evidence-based guidelines for treating depressive disorders with antidepressants: a revision of the 1993 British Association for Psychopharmacology guidelines. British Association for Psychopharmacology. J Psychopharmacol. 2000;14(1):3–20.
4. Geddes JR, Cipriani A. Selective serotonin reuptake inhibitors. BMJ. 2004;329(7470):809–10.
5. Graf H, Walter M, Metzger CD, Abler B. Antidepressant-related sexual dysfunction - perspectives from neuroimaging. Pharmacol Biochem Behav. 2014;121:138–45.
6. Brambilla P, Cipriani A, Hotopf M, Barbui C. Side-effect profile of fluoxetine in comparison with other SSRIs, tricyclic and newer antidepressants: a meta-analysis of clinical trial data. Pharmacopsychiatry. 2005;38(2):69–77.
7. Fleurence R, Williamson R, Jing Y, Kim E, Thase ME. A Systematic Review of Augmentation Strategies for Patients with Major Depressive Disorder. Psychopharmacology bulletin. 2009;42(3):57–90.
8. Rafeyan R, Papakostas GI, Jackson WC, Trivedi MH. Inadequate Response to Treatment in Major Depressive Disorder: Augmentation and Adjunctive Strategies. J Clin Psychiatry. 2020;81(3).

9. Jakobsen JC, Gluud C, Kirsch I. Should antidepressants be used for major depressive disorder? BMJ Evid Based Med. 2020;25(4):130.
10. Chisholm D, Sweeny K, Sheehan P, Rasmussen B, Smit F, Cuijpers P, et al. Scaling-up treatment of depression and anxiety: a global return on investment analysis. Lancet Psychiatry. 2016;3(5):415–24.
11. Kalynchuk LE, Pinel JP, Treit D, Kippin TE. Changes in emotional behavior produced by long-term amygdala kindling in rats. Biol Psychiatry. 1997;41(4):438–51.
12. Althammer F, Ferreira-Neto HC, Rubaharan M, Roy RK, Patel AA, Murphy A, et al. Three-dimensional morphometric analysis reveals time-dependent structural changes in microglia and astrocytes in the central amygdala and hypothalamic paraventricular nucleus of heart failure rats. J Neuroinflammation. 2020;17(1):221.
13. Salzman CD, Fusi S. Emotion, cognition, and mental state representation in amygdala and prefrontal cortex. Annu Rev Neurosci. 2010;33:173–202.
14. Zhang X, Lei B, Yuan Y, Zhang L, Hu L, Jin S, et al. Brain control of humoral immune responses amenable to behavioural modulation. Nature. 2020;581(7807):204–8.
15. Wei Y, Chang L, Hashimoto K. Molecular mechanisms underlying the antidepressant actions of arketamine: beyond the NMDA receptor. Mol Psychiatry. 2021.
16. Webster JI, Tonelli L, Sternberg EM. Neuroendocrine regulation of immunity. Annu Rev Immunol. 2002;20:125–63.
17. Stephenson J, Nutma E, van der Valk P, Amor S. Inflammation in CNS neurodegenerative diseases. Immunology. 2018;154(2):204–19.
18. Amor S, Puentes F, Baker D, van der Valk P. Inflammation in neurodegenerative diseases. Immunology. 2010;129(2):154–69.
19. Wang B, Huang X, Pan X, Zhang T, Hou C, Su WJ, et al. Minocycline prevents the depressive-like behavior through inhibiting the release of HMGB1 from microglia and neurons. Brain Behav Immun. 2020;88:132–43.
20. Grippo AJ, Johnson AK. Stress, depression and cardiovascular dysregulation: a review of neurobiological mechanisms and the integration of research from preclinical disease models. Stress. 2009;12(1):1–21.
21. Lu Y, Zhou S, Fan C, Li J, Lian Y, Shang Y, et al. Higher inflammation and cerebral white matter injury associated with cognitive deficit in asthmatic patients with depression. J Asthma. 2020:1–15.
22. Xu X, Zeng XY, Cui YX, Li YB, Cheng JH, Zhao XD, et al. Antidepressive Effect of Arctiin by Attenuating Neuroinflammation via HMGB1/TLR4- and TNF-alpha/TNFR1-Mediated NF-kappaB Activation. ACS Chem Neurosci. 2020;11(15):2214–30.
23. Liu J, Buisman-Pijlman F, Hutchinson MR. Toll-like receptor 4: innate immune regulator of neuroimmune and neuroendocrine interactions in stress and major depressive disorder. Front Neurosci. 2014;8:309.

24. Gu HF, Li N, Xu ZQ, Hu L, Li H, Zhang RJ, et al. Chronic Unpredictable Mild Stress Promotes Atherosclerosis via HMGB1/TLR4-Mediated Downregulation of PPARgamma/LXRalpha/ABCA1 in ApoE(-/-) Mice. Front Physiol. 2019;10:165.
25. Franklin TC, Wohleb ES, Zhang Y, Fogaca M, Hare B, Duman RS. Persistent Increase in Microglial RAGE Contributes to Chronic Stress-Induced Priming of Depressive-like Behavior. Biol Psychiatry. 2018;83(1):50–60.
26. Andersson U, Yang H, Harris H. Extracellular HMGB1 as a therapeutic target in inflammatory diseases. Expert Opin Ther Targets. 2018;22(3):263–77.
27. Zhao B, Li Z, Wang Y, Ma X, Wang X, Wang X, et al. Can acupuncture combined with SSRIs improve clinical symptoms and quality of life in patients with depression? Secondary outcomes of a pragmatic randomized controlled trial. Complement Ther Med. 2019;45:295–302.
28. Xu YD, Wang Y, Park GH, Yin LM, Ran J, Liu YY, et al. Non-specific physiological background effects of acupuncture revealed by proteomic analysis in normal rats. BMC Complement Altern Med. 2014;14:375.
29. Qaseem A, Barry MJ, Kansagara D, Clinical Guidelines Committee of the American College of P. Nonpharmacologic Versus Pharmacologic Treatment of Adult Patients With Major Depressive Disorder: A Clinical Practice Guideline From the American College of Physicians. Ann Intern Med. 2016;164(5):350–9.
30. Han X, Gao Y, Yin X, Zhang Z, Lao L, Chen Q, et al. The mechanism of electroacupuncture for depression on basic research: a systematic review. Chin Med. 2021;16(1):10.
31. Lu J, Shao RH, Hu L, Tu Y, Guo JY. Potential antiinflammatory effects of acupuncture in a chronic stress model of depression in rats. Neurosci Lett. 2016;618:31–8.
32. Yue N, Li B, Yang L, Han QQ, Huang HJ, Wang YL, et al. Electro-Acupuncture Alleviates Chronic Unpredictable Stress-Induced Depressive- and Anxiety-Like Behavior and Hippocampal Neuroinflammation in Rat Model of Depression. Front Mol Neurosci. 2018;11:149.
33. Le JJ, Yi T, Qi L, Li J, Shao L, Dong JC. Electroacupuncture regulate hypothalamic-pituitary-adrenal axis and enhance hippocampal serotonin system in a rat model of depression. Neurosci Lett. 2016;615:66–71.
34. Li P, Huang W, Yan YN, Cheng W, Liu S, Huang Y, et al. Acupuncture Can Play an Antidepressant Role by Regulating the Intestinal Microbes and Neurotransmitters in a Rat Model of Depression. Med Sci Monit. 2021;27:e929027.
35. Huang W, Meng X, Huang Y, Liu S, Zhu A, Li P, et al. Nitric Oxide and Cyclic Guanosine Monophosphate Signaling Mediates the Antidepressant Effects of Acupuncture in the Rat Model of Chronic Unpredictable Mild Stress. Med Sci Monit. 2019;25:9112–22.
36. Cheng WJ, Li P, Huang WY, Huang Y, Chen WJ, Chen YP, et al. Acupuncture Relieves Stress-Induced Depressive Behavior by Reducing Oxidative Stress and Neuroapoptosis in Rats. Front Behav Neurosci. 2021;15:783056.

37. Lee MJ, Ryu JS, Won SK, Namgung U, Jung J, Lee SM, et al. Effects of Acupuncture on Chronic Stress-Induced Depression-Like Behavior and Its Central Neural Mechanism. Front Psychol. 2019;10:1353.
38. Wang B, Lian YJ, Su WJ, Peng W, Dong X, Liu LL, et al. HMGB1 mediates depressive behavior induced by chronic stress through activating the kynurenine pathway. Brain Behav Immun. 2018;72:51–60.
39. Willner P, Towell A, Sampson D, Sophokleous S, Muscat R. Reduction of sucrose preference by chronic unpredictable mild stress, and its restoration by a tricyclic antidepressant. Psychopharmacology (Berl). 1987;93(3):358–64.
40. Antoniuk S, Bijata M, Ponimaskin E, Wlodarczyk J. Chronic unpredictable mild stress for modeling depression in rodents: Meta-analysis of model reliability. Neurosci Biobehav Rev. 2019;99:101–16.
41. Li ZR. Experimental Acupuncture Science Beijing, China: China Press of Traditional Chinese Medicine; 2007 [
42. Markel AL, Khusainov RA. [Method of complex recording of the behavioral and autonomic reactions of rats during conduction of the "open field" test]. Zh Vyssh Nerv Deiat Im I P Pavlova. 1976;26(6):1314–8.
43. Araujo UC, Krahe TE, Ribeiro-Carvalho A, Gomes RAA, Lotufo BM, Moreira MFR, et al. Forced swimming stress increases natatory activity of lead-exposed mice. Toxicol Res. 2021;37(1):115–24.
44. Ge F, Yang H, Lu W, Shi H, Chen Q, Luo Y, et al. Ovariectomy Induces Microglial Cell Activation and Inflammatory Response in Rat Prefrontal Cortices to Accelerate the Chronic Unpredictable Stress-Mediated Anxiety and Depression. Biomed Res Int. 2020;2020:3609758.
45. Pellow S, Chopin P, File SE, Briley M. Validation of open:closed arm entries in an elevated plus-maze as a measure of anxiety in the rat. J Neurosci Methods. 1985;14(3):149–67.
46. Shi X, Bai H, Wang J, Wang J, Huang L, He M, et al. Behavioral Assessment of Sensory, Motor, Emotion, and Cognition in Rodent Models of Intracerebral Hemorrhage. Front Neurol. 2021;12:667511.
47. Sutton LP, Orlandi C, Song C, Oh WC, Muntean BS, Xie K, et al. Orphan receptor GPR158 controls stress-induced depression. Elife. 2018;7.
48. Castagne V, Moser P, Roux S, Porsolt RD. Rodent models of depression: forced swim and tail suspension behavioral despair tests in rats and mice. Curr Protoc Neurosci. 2011;Chap. 8:Unit 8 10A.
49. Snyder JS, Soumier A, Brewer M, Pickel J, Cameron HA. Adult hippocampal neurogenesis buffers stress responses and depressive behaviour. Nature. 2011;476(7361):458–61.
50. Bai L, Zhang D, Cui TT, Li JF, Gao YY, Wang NY, et al. Mechanisms Underlying the Antidepressant Effect of Acupuncture via the CaMK Signaling Pathway. Front Behav Neurosci. 2020;14:563698.
51. Sahbaie P, Irvine KA, Liang DY, Shi X, Clark JD. Mild Traumatic Brain Injury Causes Nociceptive Sensitization through Spinal Chemokine Upregulation. Sci Rep. 2019;9(1):19500.

52. Si-yu L W-yH, An-ning Z, Yu W, Yang H, Peng L, et al. Analysis of the treatment of mentel illness by the thirteen ghost points in Thousand Golden Prescription. China Journal of Traditional Chinese Medicine Pharmacy. 2020;35(03):1395–8.
53. Chi L, Du K, Liu D, Bo Y, Li W. Electroacupuncture brain protection during ischemic stroke: A role for the parasympathetic nervous system. J Cereb Blood Flow Metab. 2018;38(3):479–91.
54. Su X, Wu Z, Mai F, Fan Z, Du S, Qian H, et al. 'Governor vessel-unblocking and mind-regulating' acupuncture therapy ameliorates cognitive dysfunction in a rat model of middle cerebral artery occlusion. Int J Mol Med. 2019;43(1):221–32.
55. Menghong J MZ. Clinical literature review of thirteen ghost points in the treatment of depression. Clinical Journal of Traditional Chinese Medicine. 2021;33(02):282–8.
56. Chen B, Hu SX, Liu BH, Zhao TY, Li B, Liu Y, et al. Efficacy and safety of electroacupuncture with different acupoints for chemotherapy-induced nausea and vomiting: study protocol for a randomized controlled trial. Trials. 2015;16:212.
57. Almeida IB, Gomes IA, Shanmugam S, de Moura TR, Magalhaes LS, de Aquino LAG, et al. Inflammatory modulation of fluoxetine use in patients with depression: A systematic review and meta-analysis. Cytokine. 2020;131:155100.
58. Todorovic N, Filipovic D. The antidepressant- and anxiolytic-like effects of fluoxetine and clozapine in chronically isolated rats involve inhibition of hippocampal TNF-alpha. Pharmacol Biochem Behav. 2017;163:57–65.
59. Liu FY, Cai J, Wang C, Ruan W, Guan GP, Pan HZ, et al. Fluoxetine attenuates neuroinflammation in early brain injury after subarachnoid hemorrhage: a possible role for the regulation of TLR4/MyD88/NF-kappaB signaling pathway. J Neuroinflammation. 2018;15(1):347.
60. Syed SA, Beurel E, Loewenstein DA, Lowell JA, Craighead WE, Dunlop BW, et al. Defective Inflammatory Pathways in Never-Treated Depressed Patients Are Associated with Poor Treatment Response. Neuron. 2018;99(5):914–24 e3.
61. Zou W, Feng R, Yang Y. Changes in the serum levels of inflammatory cytokines in antidepressant drug-naive patients with major depression. PLoS One. 2018;13(6):e0197267.
62. Pan Y, Chen XY, Zhang QY, Kong LD. Microglial NLRP3 inflammasome activation mediates IL-1beta-related inflammation in prefrontal cortex of depressive rats. Brain Behav Immun. 2014;41:90–100.
63. Harro J. Animal models of depression: pros and cons. Cell Tissue Res. 2019;377(1):5–20.
64. Dean J, Keshavan M. The neurobiology of depression: An integrated view. Asian J Psychiatr. 2017;27:101–11.
65. Lima-Ojeda JM, Rupprecht R, Baghai TC. Neurobiology of depression: A neurodevelopmental approach. World J Biol Psychiatry. 2018;19(5):349–59.
66. Zhang B, Zhong J, Gao Z. A Brain-Spleen Axis Regulates Humoral Immunity. Neurosci Bull. 2021;37(3):427–9.

67. Singh V, Roth S, Veltkamp R, Liesz A. HMGB1 as a Key Mediator of Immune Mechanisms in Ischemic Stroke. Antioxid Redox Signal. 2016;24(12):635–51.
68. Cheng Y, Pardo M, Armini RS, Martinez A, Mouhsine H, Zagury JF, et al. Stress-induced neuroinflammation is mediated by GSK3-dependent TLR4 signaling that promotes susceptibility to depression-like behavior. Brain Behav Immun. 2016;53:207–22.
69. Osimo EF, Pillinger T, Rodriguez IM, Khandaker GM, Pariante CM, Howes OD. Inflammatory markers in depression: A meta-analysis of mean differences and variability in 5,166 patients and 5,083 controls. Brain Behav Immun. 2020;87:901–9.
70. Carboni L, Becchi S, Piubelli C, Mallei A, Giambelli R, Razzoli M, et al. Early-life stress and antidepressants modulate peripheral biomarkers in a gene-environment rat model of depression. Prog Neuropsychopharmacol Biol Psychiatry. 2010;34(6):1037–48.
71. Cazareth J, Guyon A, Heurteaux C, Chabry J, Petit-Paitel A. Molecular and cellular neuroinflammatory status of mouse brain after systemic lipopolysaccharide challenge: importance of CCR2/CCL2 signaling. J Neuroinflammation. 2014;11:132.
72. Hoogland IC, Houbolt C, van Westerloo DJ, van Gool WA, van de Beek D. Systemic inflammation and microglial activation: systematic review of animal experiments. J Neuroinflammation. 2015;12:114.
73. Middeldorp J, Hol EM. GFAP in health and disease. Prog Neurobiol. 2011;93(3):421–43.
74. Hu P, Liu J, Zhao J, Qi XR, Qi CC, Lucassen PJ, et al. All-trans retinoic acid-induced hypothalamus-pituitary-adrenal hyperactivity involves glucocorticoid receptor dysregulation. Transl Psychiatry. 2013;3:e336.
75. Ulrich-Lai YM, Xie W, Meij JT, Dolgas CM, Yu L, Herman JP. Limbic and HPA axis function in an animal model of chronic neuropathic pain. Physiol Behav. 2006;88(1–2):67–76.
76. Liu S, Guo R, Liu F, Yuan Q, Yu Y, Ren F. Gut Microbiota Regulates Depression-Like Behavior in Rats Through the Neuroendocrine-Immune-Mitochondrial Pathway. Neuropsychiatr Dis Treat. 2020;16:859–69.
77. Sun Y, Bai L, Niu X, Wang Z, Yin B, Bai G, et al. Elevated Serum Levels of Inflammation-Related Cytokines in Mild Traumatic Brain Injury Are Associated With Cognitive Performance. Front Neurol. 2019;10:1120.
78. Brunson KL, Khan N, Eghbal-Ahmadi M, Baram TZ. Corticotropin (ACTH) acts directly on amygdala neurons to down-regulate corticotropin-releasing hormone gene expression. Ann Neurol. 2001;49(3):304–12.
79. van Rijzingen IM, Gispen WH, Dam R, Spruijt BM. Chronic and intra-amygdala administrations of the ACTH(4–9) analog ORG 2766 modulate behavioral changes after manipulation of NMDA-receptor activity. Brain Res. 1996;717(1–2):200–3.
80. De Kloet ER, Vreugdenhil E, Oitzl MS, Joels M. Brain corticosteroid receptor balance in health and disease. Endocr Rev. 1998;19(3):269–301.
81. Maes M, Bosmans E, Suy E, Vandervorst C, DeJonckheere C, Raus J. Depression-related disturbances in mitogen-induced lymphocyte responses and interleukin-1 beta and soluble interleukin-2 receptor

production. Acta Psychiatr Scand. 1991;84(4):379–86.
82. Jelencic V, Lenartic M, Wensveen FM, Polic B. NKG2D: A versatile player in the immune system. Immunol Lett. 2017;189:48–53.
83. Lanier LL. NKG2D Receptor and Its Ligands in Host Defense. Cancer Immunol Res. 2015;3(6):575–82.
84. Zou Y, Li S, Chen T, Li Z, Gao X, Wang Z. Astragaloside IV ameliorates peripheral immunosuppression induced by cerebral ischemia through inhibiting HPA axis. Int Immunopharmacol. 2022;105:108569.
85. Korneva EA, Shkhinek EK. [Stress and immune system function]. Usp Fiziol Nauk. 1989;20(3):3–20.
86. Shurin MR, Zhou D, Kusnecov A, Rassnick S, Rabin BS. Effect of one or more footshocks on spleen and blood lymphocyte proliferation in rats. Brain Behav Immun. 1994;8(1):57–65.
87. Khaw YM, Majid D, Oh S, Kang E, Inoue M. Early-life-trauma triggers interferon-beta resistance and neurodegeneration in a multiple sclerosis model via downregulated beta1-adrenergic signaling. Nat Commun. 2021;12(1):105.
88. Song M, Zhang J, Li X, Liu Y, Wang T, Yan Z, et al. Effects of Xiaoyaosan on Depressive-Like Behaviors in Rats With Chronic Unpredictable Mild Stress Through HPA Axis Induced Astrocytic Activities. Front Psychiatry. 2020;11:545823.

Figures

Figure 1

Experimental flowchart and body weight of 4 groups measured in 28 days. **(A)** All protocols in the study were conducted as the experimental flowchart shows. **(B)** The positions and angle of needle insertion for *Fengfu* (GV 16) and *Shangxing* (GV 23) acupoints (in bold) were performed in the study, and the headset was for assisting acupuncture. **(C)** The body weight of 4 groups in 28 days. **(D)** The comparison of body weight between groups of acupuncture and fluoxetine 28 days after CUMS and treatment. Data represents mean ± standard error of the mean ($\bar{x} \pm s$) (n=9). The P value above CUMS bar, AP bar and FX bar were obtained from: the comparison between CON and CUMS group, the comparison between AP and CUMS group, and the comparison between FX and CUMS bar. Different from CON group: *** P<0.001; different from CUMS group: $^{\#}$ P<0.05; No-CON, non-control groups; CON, control group; CUMS, chronic unpredictable mild stress group; AP, acupuncture + CUMS group; FX, fluoxetine + CUMS group. SPT, sucrose preference rate; FST, forced swim test; OFT, open field test; EPM, elevated plus maze test.

Figure 2

Effects of acupuncture on rats' depression-like behaviors measured by behavioral test. **(A)** The sucrose preference rates of four groups in SPT. **(B)** The immobility duration total of four groups in FST. The number of crossing grids **(C)**, fecal excretion times **(F)** and activity trajectory **(D)** in OFT. The activity trajectory **(E)**, time in closed arms **(G)** and time in open arms **(H)** in EPM. The blue region represents the center of field (red region) in **(D)**. The blue arms represent closed arms, while the red ones represent open arms in **(E)**. Data represents $\bar{x} \pm s$ (n=9). Different from CON group: * P<0.05, ** P<0.01, *** P<0.001. Different from CUMS group: $^{\#}$ P<0.05, $^{\#\#}$ P<0.01, $^{\#\#\#}$ P<0.001. SPT, sucrose preference rate; FST, forced swim test; OFT, open field test; EPM, elevated plus maze test.

Figure 3

Effects of acupuncture on HMGB1/TLR4 signaling pathway in amygdala. **(A)** The representative protein imagines of HMGB1 and TLR4 measured by WB. **(B)** The relative expression of HMGB1. **(C)** The relative expression of TLR4. **(D)** The representative mRNA imagines of HMGB1 and TLR4 measured by RT-PCR. To make a more beautiful layout, the loading control was reused. **(E)** The relative expression of HMGB1 mRNA. **(F)** The relative expression of TLR4 mRNA. **(G)** The representative images of HMGB1 in amygdala detected with immunofluorescence confocal microscopy under ×200 magnification. Scale bar: 100 μm. **(H)** The %area of HMGB1 in amygdala. The densitometric data in WB analyses of bands of interest and mRNA level in RT-PCR were all normalized by β-actin (lower band). Data represents $\bar{x} \pm s$ (n=3). Different from CON group: * P<0.05, ** P<0.01. Different from CUMS group: $^{\#}$ P<0.05. WB, western blotting; RT-PCR, reverse transcription-polymerase chain reaction; HMGB1, high-mobility group box 1; TLR4, toll-like receptor 4; DAPI, 4',6-diamidino-2-phenylindole; %area, portion of positive area in a total visual area.

Figure 4

Effects of acupuncture on structure and inflammation in spleen of CUMS rats. **(A)** The length (of the long side) of spleen ruled. **(B)** The weight of spleen. **(C)** The length of spleen. **(A-C)** share a same sample size (n=6 per group). **(D)** The representative protein imagines of HMGB1, TLR4, TNFα, IL1β and β-actin measured by WB. Acupuncture and fluoxetine reduced relative expression of HMGB1 **(E)**, TLR4 **(G)**, TNFα **(F)** and IL1β **(H)** in CUMS rats. **(D-H)** share a same sample size (n=3 per group). The densitometric data in WB analyses of bands of interest were normalized by β-actin (lower band). Data represents$\bar{x} \pm s$. Different from CON group: ** P<0.01, *** P<0.001. Different from CUMS group: $^{\#}$ P<0.05, $^{\#\#}$ P<0.01. TNFα, tumor necrosis factor alpha; IL1β, interleukin 1beta.

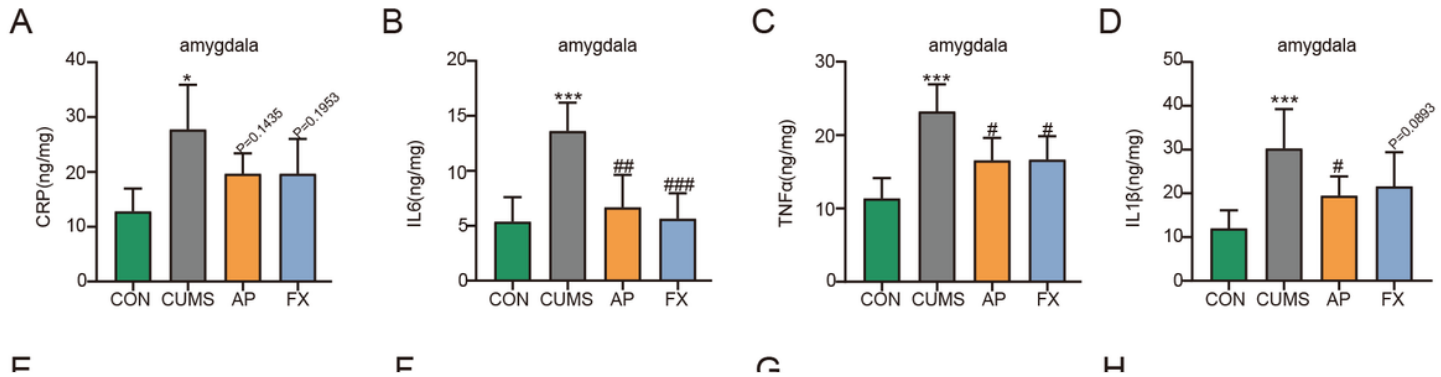

Figure 5

Effects of acupuncture on the activity of pro-inflammatory factors in amygdala and serum under CUMS. The above indexes were all detected by ELISA. The concentration of CRP, IL6, TNFα and IL1β in amygdala **(A-D)** and serum **(E-H)**. Data represents $\bar{x} \pm s$ (n=6). Different from CON group: * P<0.05, ** P<0.01, *** P<0.001. Different from CUMS group: $^{\#}$ P<0.05, $^{\#\#}$ P<0.01, $^{\#\#\#}$ P<0.001. ELISA, enzyme-linked immunosorbent assay; CRP, C reactive protein; IL6, interleukin 6.

Figure 6

Effects of acupuncture on the activity of HPA axis in amygdala and serum under CUMS. The above indexes were all detected by ELISA. The concentration of CRH, ACTH and CORT in amygdala **(A-C)** and serum **(D-F)**. Data represents $\bar{x} \pm s$ (n=6). Different from CON group: * P<0.05, ** P<0.01, *** P<0.001. Different from CUMS group: $^{\#}$ P<0.05, $^{\#\#}$ P<0.01, $^{\#\#\#}$ P<0.001. HPA, hypothalamic-pituitary-adrenal; CRH, corticotropin-releasing hormone; ACTH, adrenocorticotropic hormone; CORT, corticosterone.

Figure 7

Effects of acupuncture on the %area of IBA1 and GFAP activated by stress in amygdala. The representative images of IBA1 **(A)** and GFAP **(B)** in amygdala photoed by immunofluorescence confocal microscopy under ×200 magnification. Scale bar: 100μm. **(C)** The %area of IBA1 in amygdala. **(D)** The

%area of GFAP in amygdala. Data represents $\bar{x} \pm s$ (n=3). IBA1, ionized calcium binding adaptor molecule 1; GFAP, glial fibrillary acidic protein.

Figure 8

Effects of acupuncture on NKG2D in spleens of CUMS rats. **(A)** The representative protein imagines of NKG2D measured by WB. **(B)** The representative mRNA imagines of NKG2D measured by RT-PCR. **(C)** The relative expression of NKG2D. **(D)** The relative expression of NKG2D mRNA. Data represents $\bar{x} \pm s$ (n=3). The densitometric data in WB analyses of bands of interest and mRNA level in RT-PCR were all normalized by β-actin (lower band). Different from CON group: * P<0.05, ** P<0.01. Different from CUMS group: $^{\#\#}$ P<0.01. NKG2D, natural killer group 2 member D.

Figure 9

Schematic of antidepressant effects of acupuncture in the CUMS model. Generally, the results in our research suggest that antidepressant effects of acupuncture are processed through adjusting inflammation centrally and peripherally. Under CUMS, the HPA axis as well as HMGB1/TLR4 signaling pathway in amygdala is hyperactivated, promoting the secretion of pro-inflammatory factors, such as IL1β, IL6, TNFα and CRP in periphery and brain. What's more, microglia and astrocytes in resting state are both activated by CUMS. There is a neuronal pathway beginning in CRH-expressing neurons in amygdala and paraventricular nucleus, ending in splenic nerve in spleen, i.e., brain-spleen axis. Through brain-spleen axis, spleen can be affected by CUMS, and systemic immune function is downregulated as a low level of NKG2D, which is also an inflammatory manifestation. Further, inflammation induces depression-like behaviors in rats. However, acupuncture effectively reverses above inflammation and thus exerts a significant role in antidepressant. Red arrows indicate CUMS effects while green arrows indicate reversing effects of acupuncture.

Supplementary Files

This is a list of supplementary files associated with this preprint. Click to download.

- SupplementarymaterialsWB.docx
- Supplementarytables.docx